Spatio-temporal patterns of the effects of precipitation variability and land use/cover changes on long-term changes in sediment yield in the Loess Plateau, China

Revised manuscript submitted to *Hydrology and Earth System Sciences* (hess-2016-654)

Guangyao Gao[1,2], Jianjun Zhang[1], Yu Liu[3], Zheng Ning[1], Bojie Fu[1,2], and Murugesu Sivapalan[4,5]

[1]State Key Laboratory of Urban and Regional Ecology, Research Center for Eco-Environmental Sciences, Chinese Academy of Sciences, Beijing 100085, China
[2]Joint Center for Global Change Studies, Beijing 100875, China
[3]Key Laboratory of Ecosystem Network Observation and Modeling, Institute of Geographical Sciences and Natural Resources Research, Chinese Academy of Sciences, Beijing 100101, China
[4]Department of Geography and Geographic Information Science, University of Illinois at Urbana-Champaign, Champaign, Illinois, USA
[5]Department of Civil and Environmental Engineering, University of Illinois at Urbana-Champaign, Urbana, Illinois, USA

Correspondence to: Guangyao Gao (gygao@rcees.ac.cn)

Abstract

Within China's Loess Plateau there have been concerted revegetation efforts and engineering measures over the last 50 years aimed at reducing soil erosion and land

degradation. As a result, annual streamflow, sediment yield and sediment concentration have all decreased considerably. Human induced land use/cover change (LUCC) was the dominant factor, contributing over 70% of the sediment load reduction, whereas the contribution of precipitation was less than 30%. In this study, we use 50-year time series data (1961-2011), showing decreasing trends in the annual sediment loads of fifteen catchments, to generate spatio-temporal patterns in the effects of LUCC and precipitation variability on sediment yield. The space-time variability of sediment yield was expressed notionally as a product of two factors representing: (i) effect of precipitation and (ii) fraction of treated land surface area. Under minimal LUCC, the square root of annual sediment yield varied linearly with precipitation, with the precipitation-sediment load relationship showing coherent spatial patterns amongst the catchments. As the LUCC increased and took effect, the changes of sediment yield pattern depended more on engineering measures and vegetation restoration campaign, and the within-year rainfall patterns (especially storm events) also played an important role. The effect of LUCC is expressed in terms of a sediment coefficient, i.e., ratio of annual sediment yield to annual precipitation. Sediment coefficients showed a steady decrease over the study period, following a linear decreasing function of the fraction of treated land surface area. In this way, the study has brought out the separate roles of precipitation variability and LUCC in controlling spatio-temporal patterns of sediment yield at catchment scale.

Keywords: Loess Plateau, sediment yield, land use/land cover change, climate change, precipitation variability

1 Introduction

Streamflow and sediment transport are important controls on biogeochemical processes that govern ecosystem health in river basins (Syvitski, 2003). Changes in soil erosion on landscapes and the resulting changes in sediment transport rates in rivers have great environmental and societal consequences, particularly since they can be brought about by climatic changes and human induced land use/cover changes (LUCC) (Syvitski, 2003; Beechie et al., 2010). Understanding the dominant mechanisms behind such changes at different time and space scales is crucial to the development of strategies for sustainable land and water management in river basins (Wang et al., 2016).

In recent decades, streamflows and sediment yields in large rivers throughout the world have undergone substantial changes (Milly et al., 2005; Nilsson et al., 2005; Milliman et al., 2008; Cohen et al., 2014). Notable decreases in sediment yields have been observed in approximately 50% of the world's rivers (Walling and Fang, 2003; Syvitski et al., 2005). Many studies have investigated the dynamics of streamflows and sediment yields at different spatial and temporal scales (Mutema et al., 2015; Song et al., 2016; Gao et al., 2016; Tian et al., 2016). In addition to climate variability, LUCC, soil and water conservation measure (SWCM) and construction of reservoirs and dams have substantially contributed to the sediment load reductions (Walling, 2006; Milliman et al., 2008; Wang et al., 2011). While previous studies have certainly provided valuable insights into the streamflow and sediment load changes, the distinctive roles of LUCC and precipitation variability in changing sediment loads still need further investigation in large domains and across gradients of climate and land surface conditions (Walling, 2006; Mutema et al.,

2015). A particularly useful approach to the development of generalizable understanding of the effects of precipitation variability and LUCC is a comparative analysis approach focused on extracting spatio-temporal patterns of sediment yields based on observations in multiple locations within the same region, or even across different regions. This is especially valuable and crucial in areas with severe soil erosion and fragile ecosystems, e.g., the Loess Plateau (LP) in China. This is the motivation for the work presented in this paper.

The LP lies in the middle reaches of the Yellow River (YR) Basin, and contributes nearly 90% of the YR sediment (Wang et al., 2016). The historically severe soil erosion in the LP is due to sparse vegetation, intensive rainstorms, erodible loessial soil, steep topography and a long agricultural history (Rustomji et al., 2008). To control such severe soil erosion, several SWCMs including terrace and check-dam construction, afforestation and pasture reestablishment have been implemented since the 1950s (Yao et al., 2011; Zhao et al., 2017). A large ecological restoration campaign, the Grain-for-Green (GFG) project converting farmland on slopes exceed 15° to forest and pasture lands, was implemented in 1999 (Chen et al., 2015). Furthermore, the climate in the LP region has been showing both warming and drying trends (i.e., increased potential evapotranspiration and reduced precipitation) since the 1950s (Zhang et al., 2016).

These substantial LUCC have notably altered the hydrological regimes in the LP combined with the climate change. Consequently, the sediment yields within the LP have showed a predictable decline trend over the past 60 years (Zhao et al., 2017), resulting in approximately a 90% decrease of sediment yield in the YR (Miao et al., 2010, 2011; Wang et al., 2016). Many other studies have detected the influences of LUCC and precipitation

variability on sediment load changes within the LP. Rustomji et al. (2008) estimated that the contributions of catchment management practices to the decrease of annual sediment yield ranged between 64% and 89% for eleven catchments in the LP during 1950s-2000. Zhao et al. (2017) examined the spatio-temporal variation of sediment yield from 1957 to 2012 across the LP. Zhang et al. (2016) pointed out that the combined effects of climate aridity, engineering projects and vegetation cover change have induced significant reductions of sediment yield between 1950 and 2008. Wang et al. (2016) found that engineering measures for soil and water conservation were the main factors for the sediment load decrease between 1970s-1990s, but large-scale vegetation restoration campaigns also played an important role in reducing soil erosion since the 1990s.

On the basis of the outcomes of these previous studies, it is now generally accepted that the largest reductions of sediment yield within the LP resulted from LUCC. However, this is general knowledge covering the whole region, and given the significant variability of climate and catchment characteristics across the LP (Sun Q et al., 2015; Sun W et al., 2015), it is important to go further and explore how these might affect spatio-temporal patterns of sediment yield. Exploration of these patterns is important for sustainable ecosystem restoration and water resources planning and management within the LP. They also will serve as the basis for future research aimed at the development of more generalizable understanding of landscape and climate controls on sediment yields at the catchment scale.

Most of the sediment yield of the LP was produced in the Coarse Sandy Hilly Catchments (CSHC) region (Fig. 1) in the central region of the LP, which supplied over 70% of total sediment load in the YR, especially coarse sand (Rustomji et al., 2008). The CSHC

region was the focus of our efforts to investigate the variation of sediment load within the LP. The specific objectives of this study therefore are to: (1) attribute the temporal changes in sediment yield to changes in both precipitation variability and LUCC over the entire study period (1961-2011) within the CSHC region, (2) extract spatio-temporal trends in sediment yields on the basis of annual sediment yield data from 15 catchments within the region, (3) separate the contributions of precipitation variability and fractional area of LUCC to the observed spatio-temporal patterns of sediment yields, and pave the way for more detailed process-based studies in the future.

2 Materials and methods

2.1 Study area

The CSHC region covers the area between the Toudaoguai to Longmen hydrological stations in the mainstream of the YR (Fig. 1). The main stream that flows through the CSHC region is 733 km long and covers an area of 12.97×10^4 km^2, accounting for 14.8% of the entire YR Basin. The CSHC region is characterized by arid to semi-arid climate conditions. The annual precipitation in the CSHC region during 1961-2011 is 437 mm on average, and varied from 580 mm in the southeast to lower than 300 mm in the northwest (McVicar et al., 2007). The precipitation that occurs during the flood season (June-September) is usually in the form of rainstorms with high intensity and accounts for 72% of the annual rainfall total. Correspondingly, about 45% of the annual runoff and 88% of the annual sediment yield within the CSHC region are produced during the flood season. The northwestern part of the CSHC is relatively flat while the southeastern part is more finely dissected (Rustomji et al., 2008).

Fourteen main catchments along the north-south transect within the CSHC study area were chosen for the study (Fig. 1). These catchments account for 57.4% of the CSHC area, and contribute about 70% and 72% of streamflow and sediment load of the overall CSHC, respectively, based on observed hydrological data during 1961-2011. Characteristics of these catchments are shown in Table 1 and Fig. 2. It can be seen that the catchments present strong climate and land surface gradients. The catchments in the northwestern part (#1-6) have relatively lower mean annual precipitation (380 mm< $\overline{P}$ <445 mm, where $\overline{P}$ is mean annual precipitation over 1961-2011) and low growing season (April-October) LAI (0.41<LAI<0.48, where LAI is the leaf area index), while the corresponding values for catchments in the southeastern part (#7-14) are 470-570 mm and 0.63<LAI<3.26, respectively.

The entire CSHC region is considered as an additional "catchment" and it is also examined independently. The streamflow and sediment load for the whole CSHC region were taken to be equal to the differences of corresponding measurements between the Toudaoguai and Longmen gauging station. The average annual precipitation, streamflow and sediment load of the CSHC region during 1961-2011 was 437.27 mm, 33.30 mm and 5.17 Gt, respectively. Both the annual river discharge and sediment load across the CSHC region showed significant decreasing trends (-0.82 mm yr^{-1}, p<0.001 and -0.19 Gt yr^{-1}, p<0.001, respectively) over the past five decades, whereas precipitation decreased only slightly (-0.93 mm yr^{-1}, p=0.25) (Fig. 3).

2.2 Data

Monthly streamflow and sediment load data during 1961-2011 were provided by the

158 Yellow River Conservancy Commission of China. Daily rainfall data from 1961 to 2011 at
159 66 meteorological stations in and around the CSHC region were obtained from the National
160 Meteorological Information Center of China. The spatially average of rainfall data was
161 carried out using the co-kriging interpolation algorithm with the DEM as an additional
162 input. With the hydro-meteorological data (including annual precipitation, P [mm],
163 streamflow, Q [mm], and sediment load, S [t]), specific sediment yield defined as $SSY=S/A$
164 [t km^{-2}], where A is the drainage area of the hydrological station [km^2], sediment
165 concentration defined as $SC=S/(Q.A)$ [kg m^{-3}] and the sediment coefficient defined as
166 $C_s=SSY/P$ [t km^{-2} mm^{-1}] were estimated for each catchment.
167 The mean catchment slope based on the ASTER GDEM data with a resolution of 30 m
168 and soil data (scale 1:500,000) were provided by the National Earth System Science Data
169 Sharing Infrastructure (http://www.geodata.cn). The land use information as at 1975, 1990,
170 2000 and 2010 was determined with Landsat MSS and TM remote sensing images at a spatial
171 resolution of 30 m. Six land use types were classified, i.e., forestland, cropland, grassland,
172 construction land, water body, and barren land. The LAI data during 1982-2011 were
173 obtained from the Global Land Surface Satellite (GLASS) NDVI Series with spatial
174 resolution of 1 km (www.landcover.org, Zhao et al., 2013). The total areas impacted by
175 various SWCMs (i.e., afforestation, grass plantation, terraces and check-dams) in each
176 catchment during1960s-2000s were obtained from Yao et al. (2011).

177 **2.3 Methods**

178 **2.3.1 Trend test**

179 The non-parametric Mann-Kendall (M-K) test method proposed by Mann (1945) and

Kendall (1975) was used to determine the significance of the trends in annual meteorological and hydrological time series. A precondition for using the MK test is to remove the serial correlation of climatic and hydrological series. In this study, the trend-tree pre-whitening (TFPW) method of Yue and Wang (2002) was used to remove the auto-correlations before the trend test. There was no residual autocorrelation remaining after performing the TFPW. A *Z*-statistic was obtained from the M-K test on the whitened series. A negative value of *Z* indicates a decrease trend, and vice versa. The magnitude of the slope of the trend (β) was estimated by (Sen, 1968; Hirsch et al., 1982):

$$\beta = \text{Median}\left[\frac{x_j - x_i}{j - i}\right] \quad \text{for all } i<j \tag{1}$$

where x_i and x_j are the sequential data values in periods i and j, respectively.

2.3.2 Attribution analysis of changes in sediment yield

The time-trend analysis method was used to determine the quantitative contributions of LUCC and precipitation variability to sediment yield changes. This method is primarily designed to determine the differences in hydrological time series between different periods (reference and validation periods) with different LUCC conditions (Zhang et al., 2011). In this method, the regression equation between precipitation and sediment yield is developed and evaluated during the reference period, and the established equation is then used to estimate sediment yield during the validation period. The difference between measured and predicted sediment yields during the validation period represents the effects of LUCC, and the residual changes are caused by precipitation variability. The governing equations of the time-trend analysis method can be expressed as:

$$SSY_1 = f(P_1) \tag{2}$$

$$SSY_2' = f(P_2) \quad (3)$$

$$\Delta SSY^{\mathrm{LUCC}} = \overline{SSY_2} - \overline{SSY_2'} \quad (4)$$

$$\Delta SSY^{\mathrm{Pre}} = \left(\overline{SSY_2} - \overline{SSY_1}\right) - \Delta SSY^{\mathrm{LUCC}} \quad (5)$$

where SSY' is the predicted sediment yield, subscripts 1 and 2 indicate the reference and validation periods, respectively. $\overline{SSY_1}$ and $\overline{SSY_2}$ represent mean measured sediment yield during the reference and validation periods, respectively, and $\overline{SSY_2'}$ represents mean predicted sediment yield during the validation period. $\Delta SSY^{\mathrm{LUCC}}$ and $\Delta SSY^{\mathrm{Pre}}$ are sediment yield changes during the validation period associated with LUCC and precipitation variability, respectively. Rustomji et al. (2008) found that the square root of annual sediment yield in the catchments of the Loess Plateau was linearly related to annual precipitation. This was used in this study as the motivation to develop the precipitation-sediment yield relationship during the reference period:

$$\sqrt{SSY} = aP + b \quad (6)$$

In this study, the full data period of 1961-2011 was divided into three phases (1961-1969, 1970-1999 and 2000-2011). The first period was considered the reference period as the effects of human activities were slight and could be ignored (Wang et al., 2016). During the second stage, numerous SWCMs were implemented. For the third stage, a large ecological restoration campaign (GFG project) was launched in 1999.

3 Results and discussion

3.1 Changes of land use/cover

The CSHC region has undergone extensive LUCC caused by the implementation of SWCM and vegetation restoration projects (e.g., the GFG project). Fig. 4 shows the

224 distribution of land use types of the CSHC region in 1975, 1990, 2000 and 2010. More than
225 90% of the whole area is occupied by the cropland, forestland and grassland. The area of
226 cropland decreased by 26.72% and forestland increased by 53.15%, and there was no
227 obvious change for the area of grassland (increase of 4.21%) in the CSHC region from
228 1975-2010. The majority of changes occurred during 2000-2010 due to the GFG
229 (reforestation) project (26.67% decrease and 36.21% increase for cropland and forestland,
230 respectively). The transition from cropland to forestland was greater in the catchments of
231 the southeastern part (especially in catchments #7-#9) than that in the northwestern part
232 (Fig. 4). From 1975 to 2000, the increase of forestland was 26.34% and 4.55% in the
233 southeastern and northwestern part, respectively, and the change of cropland was negligible
234 (only -0.39% and 0.22%, respectively). During 2000-2010, the forestland increased by
235 47.79% and 18.30%, and the cropland decreased by 44.84% and 21.04% in the
236 southeastern and northwestern part, respectively.

237 The SWCMs implemented in the LP included both biotic treatments (e.g., afforestation
238 and grass-planting) and engineering measures (e.g., construction of terrace and check-dam
239 and gully control projects). Afforestation, grass-planting and construction of terraces are
240 seen as the slope measures, while building of check-dams and gully control projects are the
241 measures on the river channel. Although the utilized area of engineering measures was
242 much smaller than the biotic treatments, they can immediately and substantially trap
243 streamflow and sediment load. The fraction of the treated area (area treated by erosion
244 control measures relative to total catchment area) within the CSHC increased from 3.95%
245 in the 1960s to 28.61% in the 2000s (Fig. 5). The increase of the treated area was greatest

during the 1980s as a result of comprehensive management of small watersheds and during the 2000s due to the GFG project since 1999. Some decreases in these areas occurred during the 1990s as some of the erosion control measures undertaken were then subsequently destroyed.

The growing season LAI of the whole CSHC region changed from 0.74 during 1982-1999 to 0.81 during 2000-2011, an increase of 10.16% (Fig. 5). The LAI did not show significant increase during 1982-1999 (0.003 yr^{-1}, p=0.11), and it increased significantly during 2000-2011 (0.024 yr^{-1}, p<0.01). The increase of growing season LAI during 1982-2011 was greater for the catchments in the southeastern part (0.009 yr^{-1}) compared to the northwestern part (0.004 yr^{-1}), especially after 2000 (Fig. 6). From the period of 1982-1999 to 2000-2011, the average increase of growing LAI of the fourteen sub-catchments is 0.088 yr^{-1} (0.010-0.183 yr^{-1}), with the increase of 0.114 yr^{-1} and 0.053 yr^{-1} in the southeastern and northwestern part, respectively.

3.2 Trends of hydro-meteorological and sediment yield variables

Table 2 shows the trends in annual P, Q, SSY, SC and C_s of the fifteen catchments during 1961-2011. The annual P showed a decline trend in all catchments but is only significant in the Xinshui and Zhouchuan catchments (p<0.05). The annual Q, SSY, SC and C_s showed significant decreasing trends in all the catchments, and most of the decreases were at the 0.001 significance level. For the fourteen sub-catchments, the average decrease rates of annual values of Q, SSY, SC and C_s were 0.86 mm yr^{-1} (0.24-1.66 mm yr^{-1}), 190.06 t km^{-2} yr^{-1} (26.47-398.82 t km^{-2} yr^{-1}), 2.73 kg m^{-3} yr^{-1} (0.69-4.70 kg m^{-3} yr^{-1}) and 0.38 t km^{-2} mm^{-1} yr^{-1} (0.04-0.87 t km^{-2} mm^{-1} yr^{-1}), respectively. For the whole CSHC region, the

corresponding change rates of Q, SSY, SC and C_s were -0.85 mm yr^{-1}, -131.52 t km^{-2} yr^{-1}, -2.06 kg m^{-3} yr^{-1} and -0.27 t km^{-2} mm^{-1} yr^{-1}, respectively. The annual average reductions in the whole CSHC region are equivalent to 2.56%, 3.30%, 2.01% and 3.07% of the mean annual values of Q, SSY, SC and C_s, respectively.

The mean and the coefficient of variation, C_v, representing inter-annual variability of annual values of P, Q, SSY, SC and C_s of the fifteen catchments during the three phases (reference period-1, period-2 and period-3) are shown in Fig. 7. Compared to standard deviation, the C_v value was better able to indicate the inter-annual variability of precipitation, streamflow and sediment load among the catchments with distinct different average values. Compared to the reference period, the mean annual precipitation decreased by 11.73% (6.36%-15.69%) and 10.64% (5.88%-16.7%) on average in period-2 and period-3, respectively. From period-2 to period-3, the change of mean annual precipitation was slight (increased by 1.32% on average) with a decrease of 2.45%-5.87% in four catchments and an increase in the remaining catchments (0.35%-8.29%). The variability of annual P also decreased as indicated by the reductions of C_v values during period-2 and period-3 (Fig. 7a). In contrast to annual P, the reductions of mean annual Q, SSY, SC and C_s were clearly more evident. With respect to the reference period, the reduction was 34.41% (9.45%-54.72%), 48.02% (17.98%-67.61%), 24.20% (-9.93%-47.77%) and 39.31% (4.64%-63.5%) for Q, SSY, SC and C_s during period-2, and the decreasing rate was even more in period-3 with values of 64.82% (36.72%-84.19%), 88.23% (64.94%-97.64%), 67.81% (17.28%-91.12%) and 85.85% (63.51%-96.97%), respectively. C_v of annual Q increased in eight catchments, with the remaining ones showing decreasing trends (Fig. 7b), while C_v values for SSY, SC and C_s

290 increased in all catchments (Figs 7c-7e). The above results indicate the substantially different
291 behaviors of the changes among precipitation, streamflow and sediment load.

292 **3.3 Quantitative attribution of sediment yield decline**

293 The effects of precipitation change and LUCC on sediment yield reductions in period-2 and
294 period-3 were quantified using Eqs. (2-6) and the results are shown in Fig. 8. The analysis
295 showed that both decreased precipitation and increased area treated with erosion control
296 measures contributed to the observed sediment load reduction, and that LUCC played the
297 major role. On average, the LUCC and precipitation change contributed 74.39% and
298 25.61%, respectively, to sediment load reduction from the reference period to period-2, and
299 their contributions were, respectively, 88.67% and 11.33% to sediment load reduction from
300 the reference period to period-3, respectively. The effect of LUCC in period-3 was greater
301 than that in period-2 as the land use/cover (see Figs. 4-5) and vegetation coverage (see Fig.
302 6) had undergone substantial changes due to the ecological restoration campaigns launched
303 during period-3. From period-2 to period-3, the contribution of precipitation was negative
304 for sediment yield reduction in eleven catchments where the annual precipitation slightly
305 increased during these two periods, and thus the contribution of LUCC was larger than 100%
306 (Fig. 8c). In the remaining four catchments, the average contribution of LUCC increased to
307 83.96%.

308 In broad terms there are two factors that govern annual sediment yield of a catchment:
309 precipitation and landscape properties (soil, topography and vegetation). Precipitation is the
310 primary driver of runoff and, therefore, directly influences the sediment transport capacity
311 of streamflow and sediment yield at the catchment scale. Higher precipitation means higher

312 streamflow, which is the immediate driver of erosion and sediment transport. Landscape
313 properties not only have an impact on the volume or intensity of streamflow, but also
314 determine the erodibility of the soil. We have investigated the correlations between the
315 potential factors (precipitation, percentage area of afforestation, pasture plantation,
316 terracing, check-dams and construction land, and LAI) and sediment yield change between
317 different stages (see Table 4). It was found that check-dam construction was the dominant
318 factor for sediment yield reduction from reference period to period-2, and pasture
319 plantation and check-dam construction acted the dominant factors for sediment yield from
320 reference period to period-3. The increase of precipitation mitigated the reduction of
321 sediment yield to some degree from period-2 to period-3.

322 Based on the above results, in the reference period before LUCC took effect, the
323 variation of *SSY* mainly depends on precipitation, and any spatial patterns of *SSY* among
324 catchments may be controlled by differences in annual precipitation and land surface
325 conditions. During the validation period (period-2 and period-3) with LUCC increased and
326 took effect, *SSY* decreased considerably whereas the decrease of precipitation was
327 insignificant, LUCC contributing over 70% of the sediment yield reduction. In this case,
328 the temporal changes of *SSY* depend more on the fraction of treated surface area and
329 precipitation possibly might play a secondary role. The spatial pattern of the impacts of
330 precipitation on sediment yield is dependent on the landscape properties among catchments.
331 Guided by this framework, we next organize the data analysis to generate separate spatial
332 and temporal patterns that constitute the respective components of the spatio-temporal
333 patterns.

334 **3.4 Spatial-temporal pattern of the impacts of precipitation on sediment yield**

335 The regression equations of $\sqrt{SSY} = aP + b$ are shown in Table 3, and the spatial
336 distributions of precipitation-sediment relationships during the three stages are shown in
337 Fig. 9. During the reference period, most of the catchments showed strong correlation
338 between precipitation and sediment yield. The coefficient of determination (R^2) ranged
339 from 0.27 to 0.87, and the correlation was significant in eleven catchments (p<0.05) (Table
340 3). Overall, the regressed equations were significant for most of the catchments, and were
341 suitable for estimating the relative contributions of LUCC and precipitation variability to
342 sediment yield changes. Furthermore, the precipitation-sediment yield relationship varied
343 from catchment to catchment and showed a spatial pattern. The correlation coefficient
344 between precipitation and sediment yield was greater for catchments in the northwestern
345 part with average R^2 value of 0.75 and p value of 0.007 compared to those in the
346 southeastern part where the average R^2 and p values were 0.48 and 0.059, respectively
347 (Table 3). Based on the slopes of the regression equations between annual precipitation and
348 sediment yield, the fourteen catchments were classified into four groups (Group-1: a>0.3,
349 Group-2: 0.2<a<0.3, Group-3: 0.1<a<0.2 and Group-4: 0<a<0.1), which indicate that the
350 sediment production capability of annual precipitation is different among the catchments
351 (Fig. 9a). The four catchments in the northwestern part had the greatest slopes of a>0.3 and
352 the Shiwang catchment had the lowest slope of 0.07. Most of the catchments in the
353 southeastern part were in the second group of 0.2<a<0.3.

354 Compared to the reference period, the correlation between precipitation and sediment
355 yield during the period-2 decreased in the catchments, as indicated by the reductions of R^2

356 value in Table 3. The slope of the regression line in the period-2 decreased in most of the
357 catchments with respect to the reference period, except in some catchments (e.g., Huangfu,
358 Gushan and Kuye) with slight increase. Furthermore, the spatial patterns of the
359 precipitation-sediment yield relationship during these two periods were somewhat different
360 (Figs. 9a and 9b).. From the reference period to period-2, Jialu catchment moved from
361 Group-1 to Group-2 and five catchments moved from Group-2 to Group-3.
362 During period-3, the correlation between precipitation and sediment yield was much
363 weaker compared to that during the reference period and period-2 (Table 3). The
364 relationship between precipitation and sediment yield was non-significant in all of the
365 catchments (Table 3). The slope of the regression line during period-3 decreased sharply
366 (Table 3), and for six catchments the regression slope (five in the north-western part and
367 one in the south-eastern part) was even negative (Fig. 9c). This result indicates that the
368 sediment production capability of annual precipitation reduced greatly during period-3, and
369 the increase of precipitation amount in some catchments did not lead to an increase of
370 sediment yield. Furthermore, the spatial pattern of precipitation-sediment relationship
371 during period-3 was much different from those during the reference period and period-2
372 based on comparisons of Fig. 9c with Figs. 9a-9b. There were only three groups with two
373 catchments having regression slopes of $0.1<a<0.2$, six catchments having regression slopes
374 of $0.1<a<0.2$ and six catchments having negative regression slopes.
375 The aforementioned analysis of the precipitation-sediment yield relationship in
376 different periods clearly indicates that the impacts of precipitation on sediment yield
377 declined with time, and the impacts were different among catchments, with a clear spatial

pattern. The effects of precipitation on the sediment yield were greater in the north-western part compared to those in the south-eastern part. The decreased effects of precipitation on sediment yield with time were consistent with the significant reductions of sediment coefficient (Table 2) and the decreased contribution of precipitation to sediment load reduction (25.61% and 11.33% in period-2 and period-3, respectively). During period-2, the LUCC were mainly induced by SWCM, especially engineering measures. During period-3, the combined effects of substantial vegetation cover and conservation measures further weakened the effects of precipitation on sediment load reduction.

Differences in catchment characteristics, including land use/cover, soil properties and topography, as well as precipitation characteristics, are clearly the reason for the spatial patterns in the precipitation-sediment yield relationship (Morera et al., 2013; Mutema et al., 2015). The lower vegetation cover was the main reason for the greater effects of precipitation on sediment yield in the northwestern part. To fully explore this, the mapping of information of catchment characteristics into sediment yield models and simulations under different climate scenarios are needed (Ma et al., 2014; Achete et al., 2015). In this context, the inter-annual and intra-annual patterns of variability of precipitation, including the distribution of storm events, may also contribute to the observed spatial patterns of precipitation-sediment yield relationship.

As LUCC took effect during period-2 and period-3, and despite the much reduced role of precipitation in driving changes in sediment yield, within-year temporal rainfall patterns did play an important role in the observed changes of sediment yield, given that most of the sediment yield was produced during a few key storm events. The correlation between

sediment yield and storm events with daily precipitation amount larger than 20 mm (including storm numbers, precipitation amount of storms) in the CSHC region during different decades were investigated (see Table 5). The analysis showed that the sediment yield was significantly correlated with storm numbers in the 1960s, 1970s and 1980s (p<0.05), and precipitation amount of storms in the 1960s and 1970s (p<0.05). This result indicated the critical role of storm events in sediment yield, especially during the periods before substantial LUCC took effect.

Looking into this in more detail, taking the Yanhe catchment as an example, the precipitation amount during the rainy season (May-October when sediment load was measured) in 2003 and 2004 was 514.31 mm and 389.05 mm, respectively, whereas the sediment load in 2004 (2427.37×10^4 t) was about over four times of that in 2004 (590.04×10^4 t). As shown in Fig. 10, there were six days with precipitation amounts over 20 mm and the maximum daily precipitation amount on 25th August was 27.85 mm in 2003, and the values in 2004 were five days and 46.34 mm on 10th August. Furthermore, heavy rainfall events were distributed in every month in 2003, whereas they were concentrated in July and August in 2004. There were five evident peaks of sediment load with the sum of 1646.24×10^4 t (67.82% of annual total) in 2004, especially the one on 10th August produced 784.53×10^4 t sediment load (32.32% of annual total) (Fig. 10b). In contrast, there were three peaks of sediment load in 2003, and the maximum value was only 139.97×10^4 t (Fig. 10a). Therefore, apart from annual precipitation amounts, within-year rainfall patterns should also be considered to investigate the effects of precipitation on temporal-spatial changes of streamflow and sediment load.

3.5 Spatial-temporal pattern of the impacts of land use/cover on sediment yield

The sediment load reductions in the LP were primarily caused by the LUCC and the implementation of SWCM. The cropland area decreased 9733.91 km^2 (8.73% of region area) and the forestland area increased 7662.50 km^2 (6.87% of region area) from 1975 to 2010. Most of the increase in forestland area was converted from cropland area induced by the GFG or reforestation project. As a result of the land use change, vegetation cover increased greatly and it substantially contributed to the decreases of runoff and sediment production. The SWCMs, such as afforestation and engineering measures were the major interventions in the study area to retain precipitation and consequently reduce streamflow and sediment load. Establishing perennial vegetation cover was considered as one of the most effective measures to stabilize soils and minimize erosion (Farley et al., 2005; Liu et al., 2014). It was reported that both runoff coefficient and sediment concentration of catchments in the LP decreased significantly and linearly with the vegetation cover (Wang et al., 2016). The engineering structures mainly included creation of terrace and building of check-dams and reservoirs, which reduced flood peaks and stored water and sediment within the catchment. There were about 110, 000 check-dams in the LP which trapped about 21 billion m^3 of sediment during the past six decades (Zhao et al., 2017). Over time, the effectiveness of engineering measures decreased as they progressively fill with sediments, and vegetation restoration must in future play a greater role in control of soil erosion for the LP.

To quantify the effects of SWCM on sediment load reduction, the relationship between the decadal sediment coefficient and the fraction of area treated with erosion control measures in the 15 catchments was analysed and the results are presented in Table 6. The

decadal sediment coefficient ($\overline{SC}$) decreased linearly with the fraction of treated land surface area (A_c) in all catchments:

$$\overline{SC} = -mA_c + n \tag{7}$$

The correlation was significant in eleven catchments (p<0.05) with R^2 ranging from 0.78 to 0.99 (Table 6). The effects of SWCM on sediment load change show a spatial pattern. The correlation between sediment coefficient and conservation measures was stronger in catchments located in the north-western part compared to that in the south-eastern part (Table 6). Based on the slope of the regression equation between the sediment coefficient and fraction of the treated area, the catchments were classified into three groups in Fig. 11 (Group-1: 0.8<m<1.2, Group-2: 0.4<m<0.8 and Group-3: 0<m<0.4), which indicated that the degree of sediment load impacted by conservation measures was different among the catchments. The average m value was 0.73 and 0.37 for the catchments in the north-western and south-eastern part, respectively, Half of the catchments in the north-western part were in Group-1 and the other half were in Group-2, whereas six of the eight catchments in the south-eastern part were in Group-3 with lowest regression slope.

4 Conclusions

The Loess Plateau has undergone major changes in land use/land cover over the last 50 years as part of a concerted effort to cut back on soil erosion and land degradation and sediment yield of rivers. These included terrace and check-dam construction, afforestation, and pasture reestablishment. Over the same period the region has also experienced some reduction in rainfall, although this is relatively insignificant. Through analyses of hydrological and sediment transport data, this study has brought out the long-term

466 decreasing trends in sediment loads across fifteen large sub-catchments located in the
467 region. The study was particularly aimed at extracting spatio-temporal patterns of sediment
468 yield and attributing these patterns to the broad hydro-climatic and landscape controls.
469 Over the study period (1961-2011), the total area undergoing erosion control treatment
470 went up from only 4% to over 30%. This included to decrease of cropland by 27%, increase
471 of forestland by 53% and grassland by 4% from 1975-2010. Over the same period annual
472 precipitation decreased by not more than 10%. As a result of the erosion control measures,
473 over the entire 50-year period, there have been major reductions in streamflow (65%),
474 sediment yield (88%), sediment concentration (68%) and sediment efficiency, i.e., annual
475 sediment yield/annual precipitation (86%).
476 The observed data in the 15 study catchments also exhibits interesting spatio-temporal
477 patterns in sediment yield. The study attempted to separate the relative contributions of
478 annual precipitation and LUCC to these spatio-temporal patterns. Before LUCC took effect
479 the data indicates a linear relationship between square root of annual sediment yield and
480 annual precipitation in all 15 catchments, with highly variable slopes of the relationship
481 between the catchments, which exhibited systematic spatial patterns, in spite of some
482 scatter. As LUCC increased and took effect, the scatter increased and the slopes of the
483 sediment yield vs precipitation relationship became highly variable and lost any predictive
484 power. The study then looked at the controls on sediment coefficient instead of sediment
485 yield (thus eliminating the effect of precipitation and enabling a direct focus on landscape
486 controls). The results of this analysis found that sediment coefficient was heavily
487 dependent on the area under land use/cover treatment, exhibiting a linear (decreasing)

relationship. Even here, there was a considerable variation in the slope of the relationship between the 15 catchments, which exhibited a systematic spatial pattern.

Preliminary analyses presented in this study suggest that much of the sediment yield in the LP may be caused during only a few major storms. Therefore, the seasonality and intra-annual variability of precipitation may play important roles in annual sediment yield, which may also explain the spatial patterns of sediment yield and the effects of the various LUCC. Also, the precipitation threshold for producing sediment yield would have increased greatly as a result of SWCM and vegetation restoration in the LP. Exploration of these questions in detail will require a more physically based model that can account for fine scale rainfall variability and catchment characteristics. This is the next immediate step in our investigations, and will be reported on in the near future.

Acknowledgements

This research was funded by the National Key Research and Development Program of China (no. 2017YFA0604703), the National Natural Science Foundation of China (no. 41471094), the Chinese Academy of Sciences (no. GJHZ 1502) and the Youth Innovation Promotion Association CAS (no. 2016040). We thank the Ecological Environment Database of Loess Plateau, the Yellow River Conservancy Commission, and the National Meteorological Information Center for providing the hydrological and meteorological data. We thank the two anonymous reviews for their valuable comments which greatly improve the quality of this manuscript.

References

Achete, F.M., van der Wegen, M., Roelvink, D., and Jaffe, B.: A 2-D process-based model for suspended sediment dynamics: a first step towards ecological modeling, Hydrol. Earth Syst. Sci., 19, 2837-2857, 2015.

Beechie, T. J., Sear, D.A., Olden, J.D., Pess, G.R., Buffington, J.M., Moir, H., Roni, P., and Pollock, M.M.: Process-based principles for restoring river ecosystems, Bioscience, 60, 209-222, 2010.

Chen, Y.P., Wang, K.B., Lin, Y.S., Shi, W.Y., Song, Y., and He, X.H.: Balancing green and grain trade, Nat. Geosci., 8, 739-741, 2015.

Cohen, S., Kettner, A.J., and Syvitski, J.P.M.: Global suspended sediment and water discharge dynamics between 1960 and 2010: continental trends and intra-basin sensitivity, Glob. Planet. Chang., 115, 44-58, 2014.

Farley, K.A., Jobbágy, E.G., and Jackson, R.B.: Effects of afforestation on water yield: a global synthesis with implications for policy, Glob. Chang. Biol., 11, 1565-1576, 2005.

Hirsch, R.M., Slack, J.R., and Smith, R.A.: Techniques of trend analysis for monthly water quality data, Water Resour. Res., 18, 107-121, 1982.

Kendall, M.G.: Rank Correlation Measures, Charles Griffin, London, UK, 1975.

Liu, X.Y., Yang, S.T., Dang, S.Z., Luo, Y., Li, X.Y., and Zhou X.: Response of sediment yield to vegetation restoration at a large spatial scale in the Loess Plateau, Sci. China Tech. Sci., 57, 1482-1489, 2014

Mann, H.B.: Nonparametric tests against trend, Econometrica, 13(3), 245-259, 1945.

Ma, X., Lu, X.X., van Noordwijk, M., Li, J.T., and Xu, J.C.: Attribution of climate change,

vegetation restoration, and engineering measures to the reduction of suspended sediment in the Kejie catchment, southwest China, Hydrol. Earth Syst. Sci., 18, 1979-1994, 2014.

McVicar, T.R., Li, L.T., Van Niel, T.G., Zhang, L., Li, R., Yang, Q.K., Zhang, X.P., Mu, X.M., Wen, Z.M., Liu, W.Z., Zhao, Y.A., Liu, Z.H, and Gao, P.: Developing a decision support tool for China's re-vegetation program: simulating regional impacts of afforestation on average annual streamflow in the Loess Plateau, For. Ecol. Manag., 251, 65-81, 2007.

Miao, C.Y., Ni, J.R., and Borthwick, A.G.L.: Recent changes of water discharge and sediment load in the Yellow River basin, China, Prog. Phys. Geogr., 34, 541-561, 2010.

Miao, C.Y., Ni, J.R., Borthwick, A.G.L, and Yang, L.: A preliminary estimate of human and natural contributions to the changes in water discharge and sediment load in the Yellow River, Glob. Planet. Chang., 76, 196-205, 2011.

Milliman, J.D., Farnsworth, K.L., Jones, P.D., Xu, K.H., and Smith, L.C.: Climatic and anthropogenic factors affecting river discharge to the global ocean, 1951-2000, Glob. Planet. Chang., 62, 187-194, 2008.

Milly, P.C.D., Dunne, K.A., and Vecchia, A.V.: Global pattern of trends in streamflow and water availability in a changing climate, Nature, 438, 347-350, 2005.

Morera, S.B., Condom, T., Vauchel, P., Guyot, J.-L., Galvez, C., and Crave, A.: Pertinent spatio-temporal scale of observation to understand suspended sediment yield control factors in the Andean region: the case of the Santa River (Peru), Hydrol. Earth Syst. Sci., 17, 4641-4657, 2013.

Mutema, M., Chaplot, V., Jewitt, G., Chivenge, P., and Blöschl, G.: Annual water, sediment, nutrient, and organic carbon fluxes in river basins: A global meta-analysis as a function

554 of scale, Water Resour. Res., 51, doi:10.1002/2014WR016668, 2015.
555 Nilsson, C., Reidy, C.A., Dynesius, M., and Revenga, C.: Fragmentation and flow regulation
556 of the world's large river systems, Science, 308, 405-408, 2005.
557 Rustomji, P., Zhang, X.P., Hairsine, P.B., Zhang, L., and Zhao J.: River sediment load and
558 concentration responses to changes in hydrology and catchment management in the
559 Loess Plateau of China, Water Resour. Res., 44, W00A04, doi:10.1029/2007WR006656,
560 2008.
561 Sen, P.K., 1968. Estimates of the regression coefficient based on Kendall's tau, J. Am. Stat.
562 Assoc., 63, 1379-1389.
563 Song, C.L., Wang, G.X., Sun, X.Y., Chang, R.Y., and Mao, T.X.: Control factors and scale
564 analysis of annual river water, sediments and carbon transport in China, Sci. Rep.,
565 6:25963, doi:10.1038/srep25963, 2016.
566 Sun, Q.H., Miao, C.Y., Duan, Q.Y., and Wang, Y.F.: Temperature and precipitation changes
567 over the Loess Plateau between 1961 and 2011, based on high-density gauge
568 observations, Glob. Planet. Chang., 132, 1-10, 2015.
569 Sun, W.Y., Song, X.Y., Mu, X.M., Gao, P., Wang, F., and Zhao, G.J.: Spatiotemporal
570 vegetation cover variations associated with climate change and ecological restoration in
571 the Loess Plateau, Agric. For. Meteorol., 209, 87-99, 2015.
572 Syvitski, J.P.M.: Supply and flux of sediment along hydrological pathways: Research for the
573 21st century, Glob. Planet. Chang., 39, 1-11, 2003.
574 Syvitski, J.P.M., Vörösmarty, C.J., Kettner, A.J., and Green, P.: Impact of humans on the flux
575 of terrestrial sediment to the global coastal ocean, Science, 308, 376-380, 2005.

576 Walling, D.E. and Fang, D.: Recent trends in the suspended sediment loads of the world
577 rivers, Glob. Planet. Chang., 39, 111-126, 2003.
578 Walling, D.E.: Human impact on land-ocean sediment transfer by the world's rivers,
579 Geomorphology, 79, 192-216, 2006.
580 Wang, H.J., Saito, Y., Zhang, Y., Bi, N.S., Sun, X.X., and Yang, Z.S.: Recent changes of
581 sediment flux to the western Pacific Ocean from major rivers in east and south-east Asia,
582 Earth Sci. Rev., 108, 80-100, 2011.
583 Wang, S., Fu, B., Piao, S., Lü, Y., Philippe, C., Feng, X., and Wang, Y.: Reduced sediment
584 transport in the Yellow River due to anthropogenic changes, Nat. Geosci., 9, 38-41,
585 2016.
586 Yao, W.Y., Xu, J.H., and Ran, D.C.: Assessment of Changing Trends in Streamflow and
587 Sediment Fluxes in the Yellow River Basin, Yellow River Water Conservancy Press,
588 Zhengzhou, China, 2011 (in Chinese).
589 Yue, S. and Wang, C.Y.: Applicability of pre-whitening to eliminate the influence of serial
590 correlation on the Mann-Kendall test, Water Resour. Res., 38, 1068,
591 doi:10.1029/2001WR000861, 2002.
592 Zhang, B.Q., He, C.S., Burnham, M., and Zhang, L.H.: Evaluating the coupling effects of
593 climate aridity and vegetation restoration on soil erosion over the Loess Plateau in China,
594 Sci. Total Environ., 539, 436-449, 2016.
595 Zhang, L., Zhao, F.F., Chen, Y., and Dixon, R.N.M.: Estimating effects of plantation
596 expansion and climate variability on streamflow for catchments in Australia, Water
597 Resour. Res., 47, W12539, doi:10.1029/2011WR010711, 2011.

598 Zhao, G.J., Mu, X.M., Jiao, J.Y., An, Z.F., Klik, A., Wang, F., Jiao, F., Yue, X.L., Gao, P., and
599 Sun, W.Y.: Evidence and causes of spatiotemporal changes in runoff and sediment yield
600 on the Chinese Loess Plateau, Land Degrad. Dev., 28, 579-590, 2017.
601 Zhao, X., Liang, S.L., Liu, S.H., Yuan,W.P., Xiao, Z.Q., Liu, Q., Cheng, J., Zhang, X.T., Tang,
602 H.R., Zhang, X., Liu, Q., Zhou, G.Q., Xu, S., Yu, K.: The global land surface satellite
603 (GLASS) remote sensing data processing system and products, Remote Sens., 5,
604 2436-2450, 2013.
605

606 **Figure captions**

607 **Figure 1.** Location of the studied catchments in the Coarse Sandy Hilly Catchments
608 (CSHC) region within the Loess Plateau.

609 **Figure 2.** Spatial distribution of (a) annual precipitation (1961-2011), (b) growing season
610 leaf area index (LAI, 1982-2011), (c) soil type and (d) slope in the study area.

611 **Figure 3.** Annual precipitation, streamflow and sediment load for the whole CSHC region
612 during 1961-2011.

613 **Figure 4.** Land use and cover of the study area in (a) 1975, (b) 1990, (c) 2000 and (d)
614 2010.

615 **Figure 5.** The changes of soil and water conservation measures area and growing season
616 LAI in the study area.

617 **Figure 6.** Long-term trends in growing season LAI changes over (a) 1982-2011, (b)
618 1982-1999 and (c) 2000-2011 in the study area. Inset in each figure shows the
619 frequency distribution of the LAI trends.

620 **Figure 7.** The changes of (a) precipitation, (b) streamflow, (c) sediment yield, (d) sediment
621 concentration and (e) sediment coefficient during different stages (1961-1969,
622 1970-1999 and 2000-2011).

623 **Figure 8.** Contributions of precipitation and land use/cover to reductions of sediment load
624 from (a) reference period (P1) to period-2 (P2), (b) reference period (P1) to period-3 (P3)
625 and (c) period-2 (P2) to period-3 (P3).

626 **Figure 9.** Spatial distribution of slope a in the regression equation $\sqrt{SSY} = aP + b$ during
627 (a) reference period (1961-1969), (b) period-2 (1970-1999) and (c) period-3

628 (2000-2011). *SSY* is specific sediment yield, and *P* is precipitation.

629 **Figure 10.** Daily precipitation and sediment load of the Yanhe catchment during rainy

630 season (May-October) in (a) 2003 and (b) 2004.

631 **Figure 11.** Spatial distribution of slope *m* in the regression equation $\overline{SC} = -mA_c + n$. $\overline{SC}$ is

632 the decadal average sediment coefficient, and A_c is the percentage of the area affected by

633 soil and water conservation measures in the catchments.

Table 1. Long-term hydrometeorological characteristics (1961-2011) and growing season leaf area index (LAI) (1982-2011) of the studied catchments in the Loess Plateau.

ID	Catchment	Gauging station	Slope (º)	Area (km^2)	Annual average					
					P (mm)	Q (mm)	SSY ($t\ km^{-2}$)	SC ($kg\ m^{-3}$)	C_s ($t\ km^{-2}\ mm^{-1}$)	LAI
1	Huangfu	Huangfu	7.8	3175	388.95	36.34	11608.86	275.90	27.35	0.412
2	Gushan	Gaoshiya	9.8	1263	422.49	49.55	12398.68	189.57	25.98	0.440
3	Kuye	Wenjiachuan	6.3	8515	394.63	59.25	9099.60	114.99	21.17	0.427
4	Tuwei	Gaojiachuan	5.8	3253	402.82	97.53	4454.47	38.44	10.16	0.406
5	Jialu	Shenjiawan	10.4	1121	445.51	49.22	9645.19	142.19	20.03	0.480
6	Wuding	Baijiachuan	6.8	29662	384.32	36.39	3089.61	74.09	7.67	0.460
7	Qingjian	Yanchuan	15.9	3468	485.58	38.93	8747.17	190.57	17.35	0.626
8	Yanhe	Ganguyi	16.5	5891	516.09	34.08	6604.90	166.31	12.45	0.920
9	Shiwang	Dacun	15.2	2141	572.16	32.99	798.89	20.32	1.31	3.261
10	Qiushui	Linjiaping	13.0	1873	469.02	34.83	7818.21	185.79	15.75	0.938
11	Sanchuan	Houdacheng	14.6	4102	486.23	50.37	3444.56	53.39	6.63	1.887
12	Quchan	Peigou	14.6	1023	539.73	30.24	7492.57	192.01	13.68	0.934
13	Xinshui	Daning	14.0	3992	529.96	29.22	3004.96	86.81	5.23	1.752
14	Zhouchuan	Jixian	15.3	436	530.06	30.13	4951.15	107.99	8.55	1.165
15	CSHC	Toudaoguai and Longmen		129654	437.27	33.30	3988.04	102.42	8.73	0.765

Table 2. Mann-Kendall trend analysis results for the annual precipitation (*P*), streamflow (*Q*), specific sediment yield (*SSY*), sediment concentration (*SC*), sediment coefficient (C_s) during 1961-2011.

ID	Catchment	*P*		*Q*		*SSY*		*SC*		C_s	
		Z	β (mm yr^{-1})	*Z*	β (mm yr^{-1})	*Z*	β (t km^{-2} yr^{-1})	*Z*	β (kg m^{-3} yr^{-1})	*Z*	β (t km^{-2} mm^{-1} yr^{-1})
1	Huangfu	-0.57^{ns}	-0.52	-4.82***	-0.99	-4.50***	-323.24	-1.97*	-2.58	-4.71***	-0.80
2	Gushan	-0.78^{ns}	-1.16	-5.02***	-1.47	-4.90***	-398.82	-3.75***	-3.92	-5.15***	-0.87
3	Kuye	-0.49^{ns}	-0.37	-5.98***	-1.66	-5.41***	-288.83	-4.61***	-3.22	-5.60***	-0.63
4	Tuwei	-0.24^{ns}	-0.27	-7.88***	-1.57	-5.20***	-130.34	-4.37***	-0.98	-5.59***	-0.30
5	Jialu	0.19^{ns}	0.26	-7.55***	-1.42	-5.36***	-298.10	-3.80***	-3.89	-5.60***	-0.69
6	Wuding	-0.39^{ns}	-0.37	-6.60***	-0.54	-4.55***	-79.19	-3.33***	-1.35	-4.94***	-0.20
7	Qingjian	-0.73^{ns}	-0.56	-2.06*	-0.24	-3.01**	-138.54	-3.09**	-3.53	-2.73**	-0.30
8	Yanhe	-1.19^{ns}	-1.17	-3.22**	-0.34	-3.36***	-115.18	-3.30***	-3.07	-3.10**	-0.22
9	Shiwang	-1.20^{ns}	-1.50	-4.01***	-0.61	-6.26***	-26.47	-5.43***	-0.69	-6.12***	-0.04
10	Qiushui	-0.28^{ns}	-0.35	-5.80***	-0.97	-6.98***	-290.44	-5.00***	-4.00	-5.98***	-0.55
11	Sanchuan	-1.43^{ns}	-1.71	-6.09***	-0.96	-5.35***	-108.69	-5.13***	-1.60	-5.99***	-0.21
12	Quchan	-0.94^{ns}	-1.14	-3.23**	-0.42	-3.65***	-173.16	-3.72***	-4.12	-3.46***	-0.29
13	Xinshui	-2.37*	-2.71	-5.57***	-0.70	-5.92***	-106.30	-3.77***	-1.92	-5.60***	-0.19
14	Zhouchuan	-2.21*	-2.48	-7.20***	-0.79	-5.86***	-183.49	-6.73***	-4.70	-7.12***	-0.35
15	CSHC	-0.67^{ns}	-0.55	-5.91***	-0.85	-5.70***	-131.52	-4.26***	-2.06	-5.67***	-0.27

[a] ***, ** and * indicate the significance levels of 0.001, 0.01 and 0.05, respectively. ns indicates the significance levels exceeds 0.05.

Table 3. The linear regression equations between square root of specific sediment yield and annual precipitation ($\sqrt{SSY} = aP + b$) during three stages (1961-1969, 1970-1999 and 2000-2011).

ID	Catchment	Reference period (1961-1969)			Period-2 (1970-1999)			Period-3 (2000-2011)		
		Regression equation	R^2	p	Regression equation	R^2	p	Regression equation	R^2	p
1	Huangfu	y = 0.341x+12.041	0.78	0.002	y = 0.397x-11.454	0.40	0.000	y = 0.135x+5.842	0.12	0.277
2	Gushan	y =0.349x+8.237	0.84	0.001	y = 0.354x-5.627	0.37	0.000	y = 0.076x+10.415	0.09	0.344
3	Kuye	y = 0.323x+9.939	0.67	0.007	y = 0.325x-3.904	0.35	0.001	y = 0.037x+8.208	0.03	0.564
4	Tuwei	y = 0.218x+12.635	0.87	0.000	y = 0.188x+1.648	0.22	0.008	y = -0.030x+27.644	0.03	0.613
5	Jialu	y = 0.382x+6.976	0.78	0.004	y = 0.222x+11.867	0.13	0.049	y = 0.072x+7.131	0.03	0.616
6	Wuding	y = 0.174x+20.544	0.53	0.027	y = 0.151x+7.546	0.26	0.004	y = 0.107x−1.511	0.17	0.182
7	Qingjian	y = 0.232x+20.923	0.48	0.040	y = 0.173x+29.319	0.16	0.027	y = 0.096x+8.344	0.05	0.522
8	Yanhe	y = 0.243x+0.741	0.39	0.070	y = 0.126x+32.699	0.16	0.031	y = 0.006x+39.338	0.00	0.973
9	Shiwang	y = 0.070x+10.935	0.27	0.150	y = 0.079x-7.837	0.24	0.006	y = -0.007x+9.426	0.01	0.769
10	Qiushui	y = 0.257x+30.738	0.60	0.014	y = 0.239x-2.814	0.29	0.002	y = -0.111x+72.39	0.06	0.448
11	Sanchuan	y = 0.191x+15.053	0.36	0.089	y = 0.174x-9.652	0.42	0.000	y = -0.056x+37.680	0.06	0.432
12	Quchan	y = 0.202x+34.590	0.72	0.016	y = 0.132x+29.685	0.09	0.104	y = -0.199x+119.247	0.11	0.300
13	Xinshui	y = 0.202x−6.593	0.71	0.004	y = 0.184x−17.464	0.53	0.000	y = 0.015x+16.822	0.01	0.823
14	Zhouchuan	y = 0.207x+20.226	0.33	0.090	y = 0.245x−31.399	0.32	0.001	y = -0.035x+26.145	0.06	0.460
15	CSHC	y = 0.218x+5.689	0.70	0.005	y = 0.174x+2.912	0.35	0.001	y = 0.001x+24.996	0.00	0.994

Table 4. The regression models for sediment yield change (Δ*SSY*) in different stages.

Period	Regression model	R^2	*p*
Reference period vs. Period-2	Δ*SSY*=-0.135-0.850 ×ΔDam	0.886	0.000
Reference period vs. Period-3	Δ*SSY*=-0.067-0.659 ×ΔDam-0.081 ×ΔPasture	0.928	0.023
Period-2 vs. Period-3	Δ*SSY*=-0.105-0.488 ×ΔDam+0.058×Δ*P*-0.129 ×ΔPasture	0.905	0.003

ΔDam and ΔPasture are changes in percentage area of check-dams and pasture plantation, respectively. Δ*P* is changes of annual precipitation over the two compared periods.

Table 5. Pearson correlation coefficients (r) and two-tailed significance test values (p) between sediment yield and annual precipitation (P), number of storms (N_{storm}) and precipitation amount of storms (P_{storm}) during different decades of the CSHC region.

Decades	P		N_{storm}		P_{storm}	
	r	p	r	p	r	p
1960s	0.772	0.015*	0.808	0.008**	0.718	0.029*
1970s	0.266	0.458	0.714	0.020*	0.695	0.026*
1980s	0.775	0.009**	0.633	0.050*	0.527	0.117
1990s	0.865	0.001***	0.591	0.072	0.572	0.084
2000s	0.118	0.715	0.006	0.986	0.138	0.669

***, ** and * indicate the significance levels of 0.001, 0.01 and 0.05, respectively.

Table 6. Regression equations between the decadal sediment coefficient and percentage of the area affected by soil and water conservation measures ($\overline{SC} = -mA_c + n$) in the catchments.

ID	Catchment	Regression equation	R^2	p
1	Huangfu	y = -0.67x+45.88	0.85	0.025
2	Gushan	y = -0.90x+46.66	0.82	0.034
3	Kuye	y = -0.83x+38.32	0.89	0.017
4	Tuwei	y =-0.48x+19.94	0.98	0.002
5	Jialu	y = -1.20x+53.20	0.97	0.002
6	Wuding	y =-0.31x+16.92	0.97	0.003
7	Qingjian	y = -0.31x+24.70	0.48	0.193
8	Yanhe	y = -0.26x+18.54	0.79	0.045
9	Shiwang	y = -0.15x+3.01	0.87	0.020
10	Qiushui	y = -0.87x+35.69	0.80	0.040
11	Sanchuan	y = -0.28x+13.32	0.78	0.046
12	Quchan	y = -0.29x+21.02	0.52	0.169
13	Xinshui	y = -0.20x+8.63	0.72	0.069
14	Zhouchuan	y = -0.61x+17.89	0.61	0.118
15	CSHC	y = -0.54x+17.74	0.99	0.000

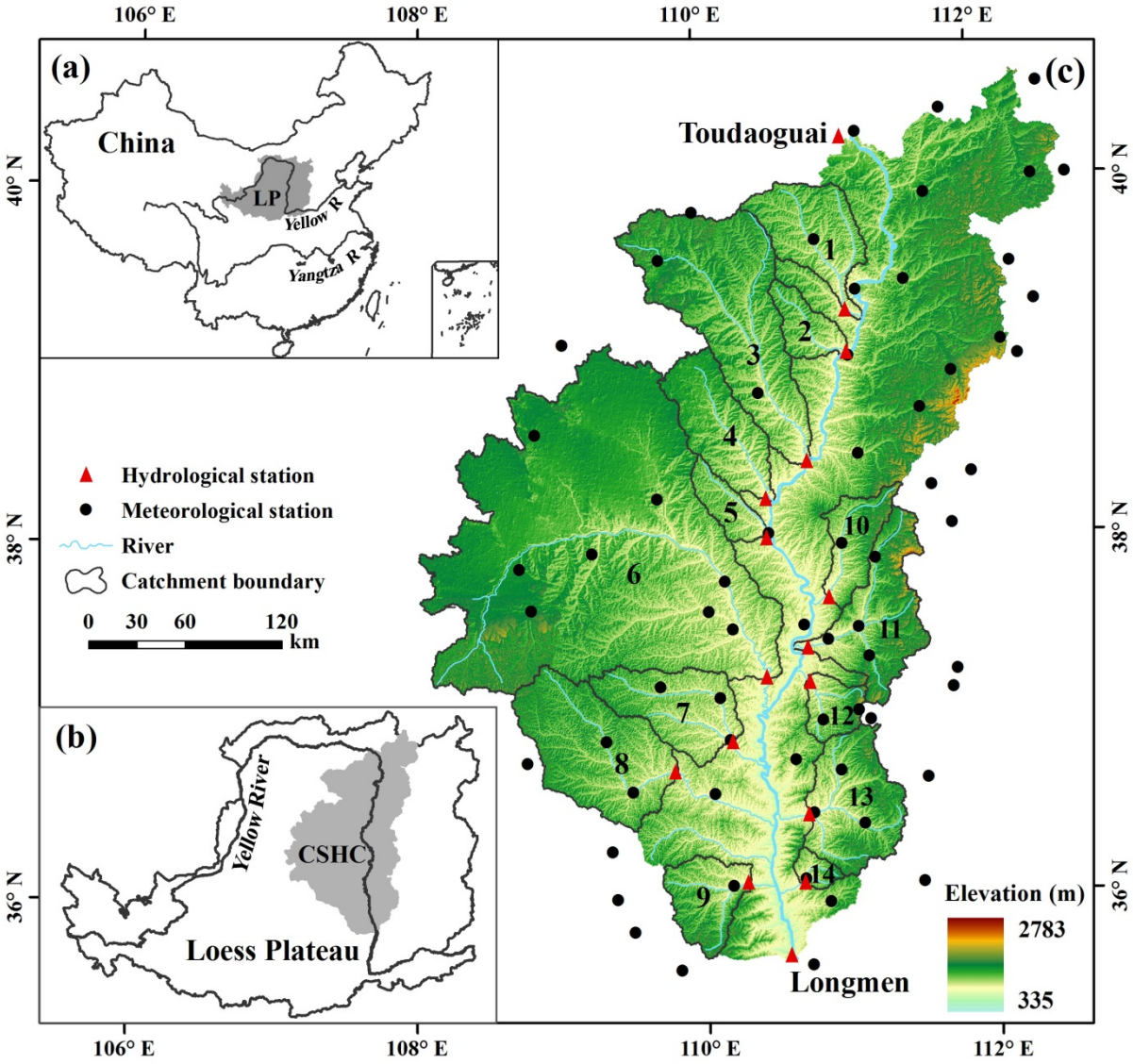

Figure 1. Location of the studied catchments in the Coarse Sandy Hilly Catchments (CSHC) region within the Loess Plateau.

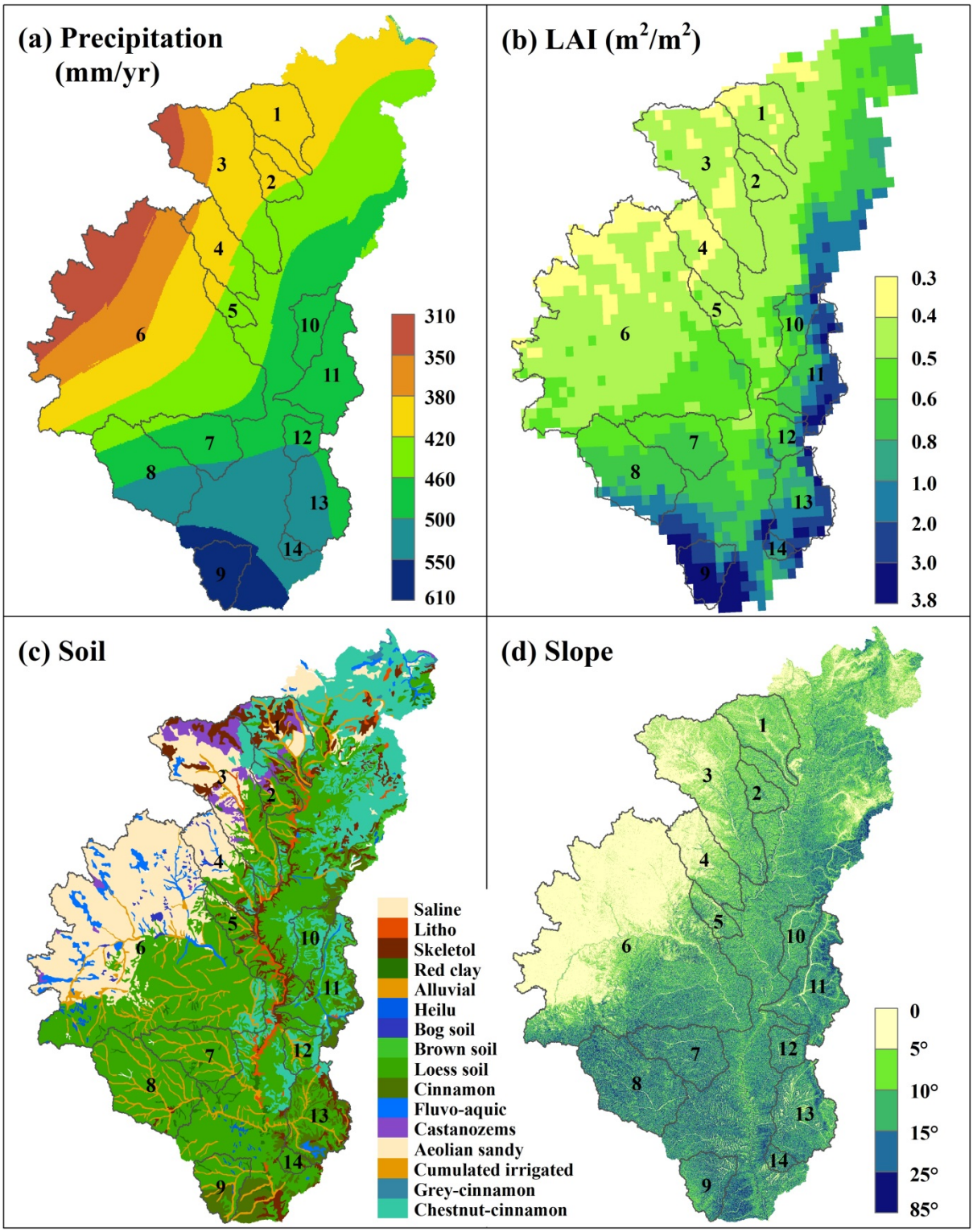

Figure 2. Spatial distribution of (a) annual mean precipitation (1961-2011), (b) growing season leaf area index (LAI, 1982-2011), (c) soil type and (d) slope in the study area.

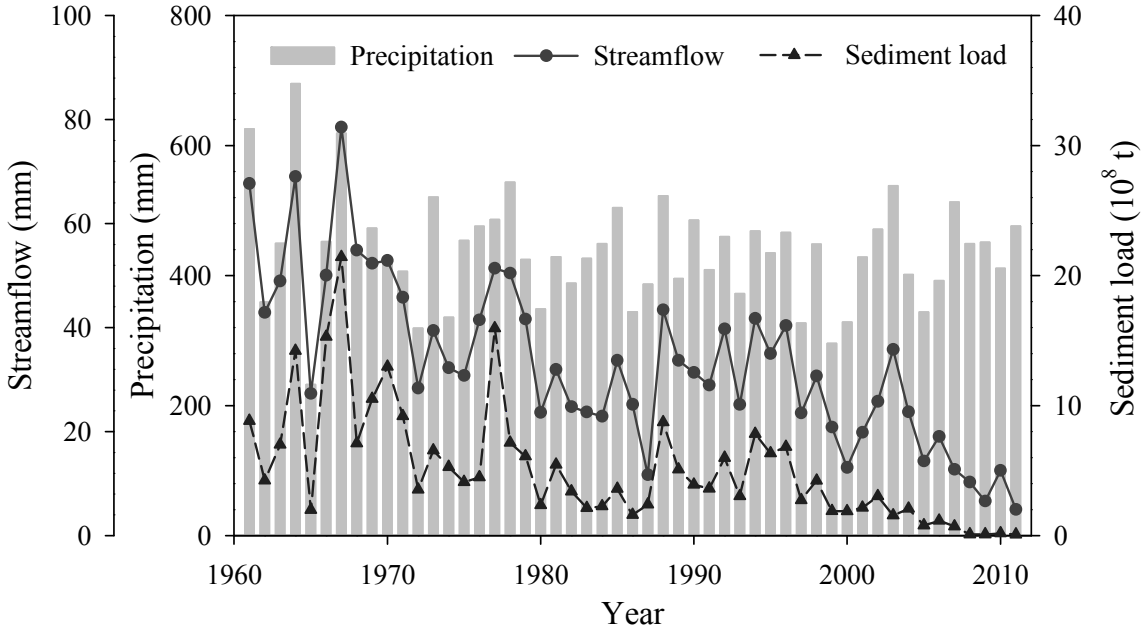

Figure 3. Annual precipitation, streamflow and sediment load for the whole CSHC region during 1961-2011.

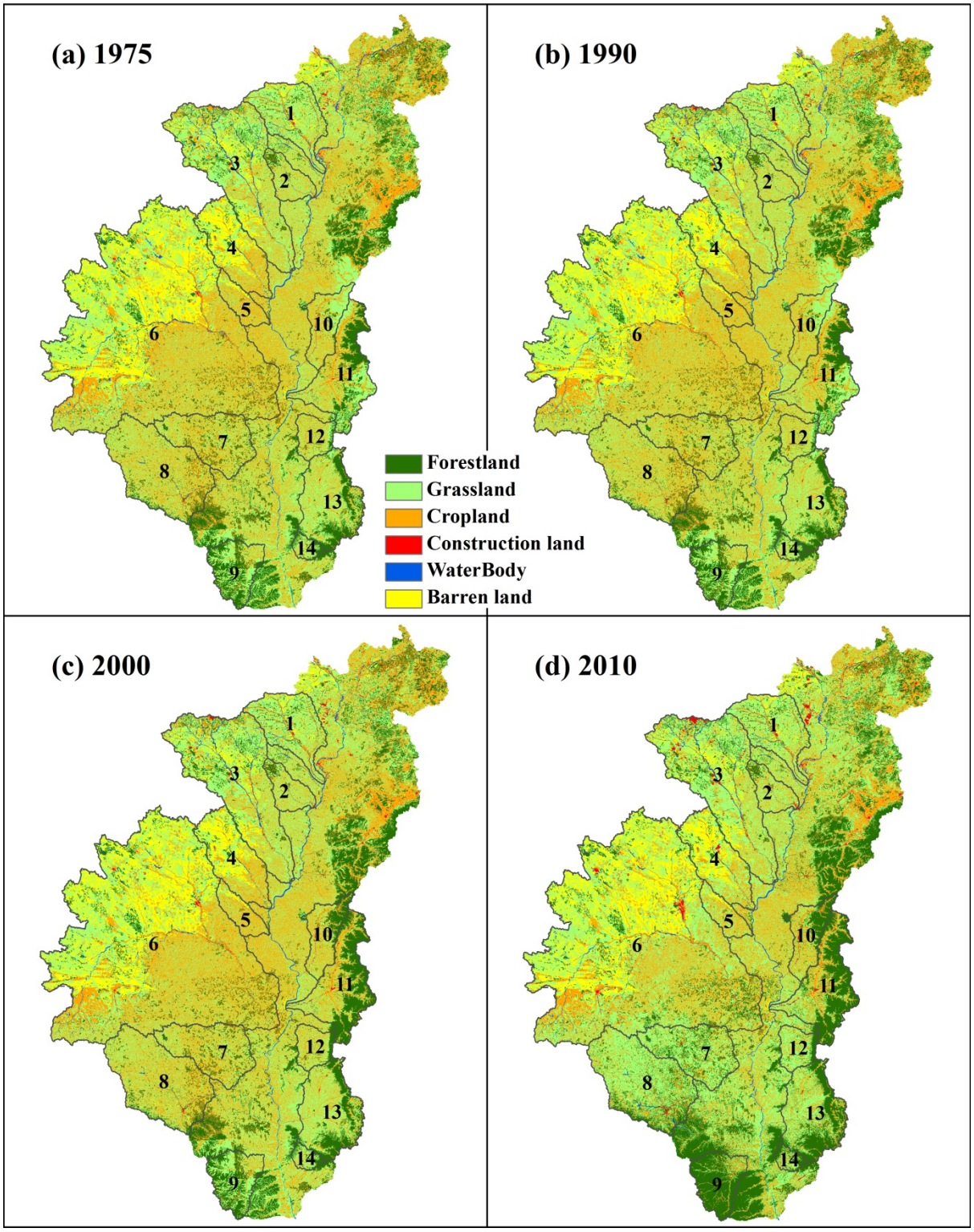

Figure 4. Land use and cover of the study area in (a) 1975, (b) 1990, (c) 2000 and (d) 2010.

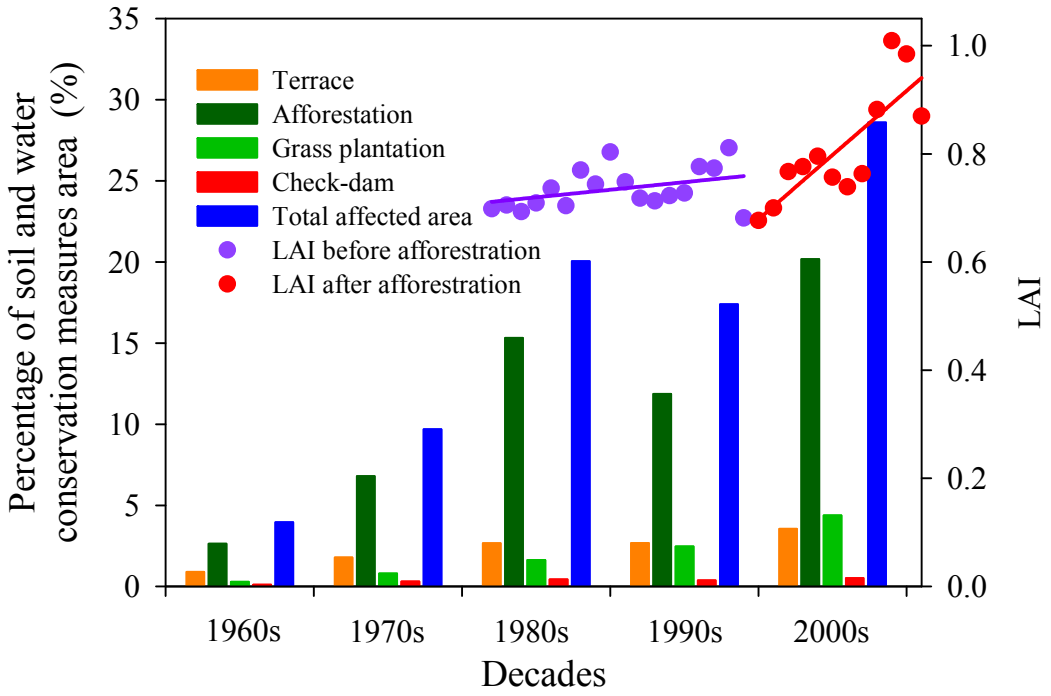

Figure 5. The changes of soil and water conservation measures area and growing season LAI in the study area.

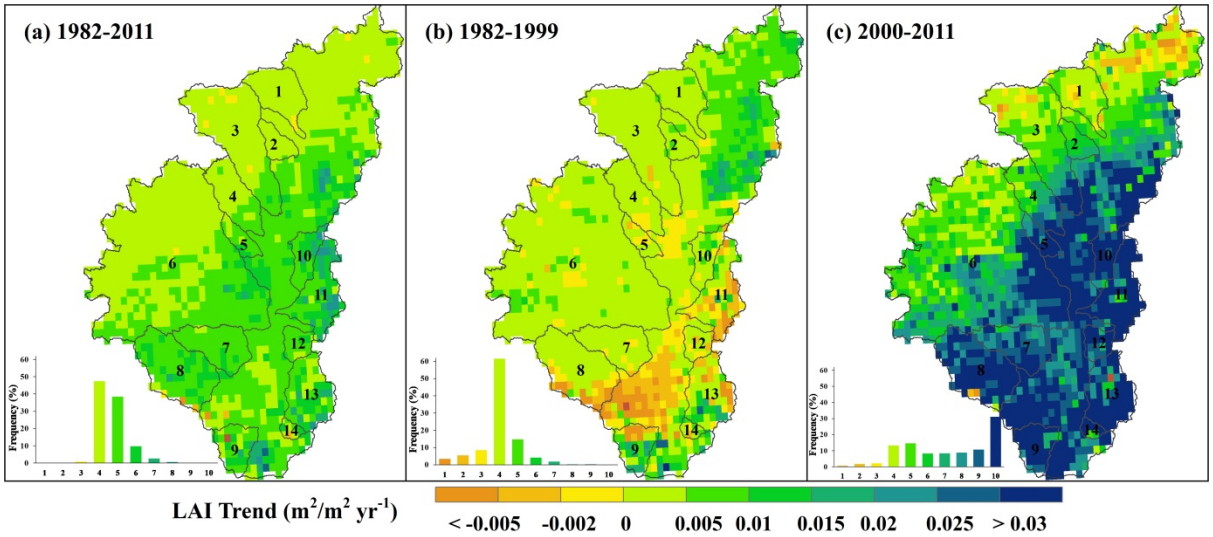

Figure 6. Long-term trends in growing season LAI changes over (a) 1982-2011, (b) 1982-1999 and (c) 2000-2011 in the study area. Inset in each figure shows the frequency distribution of the LAI trends.

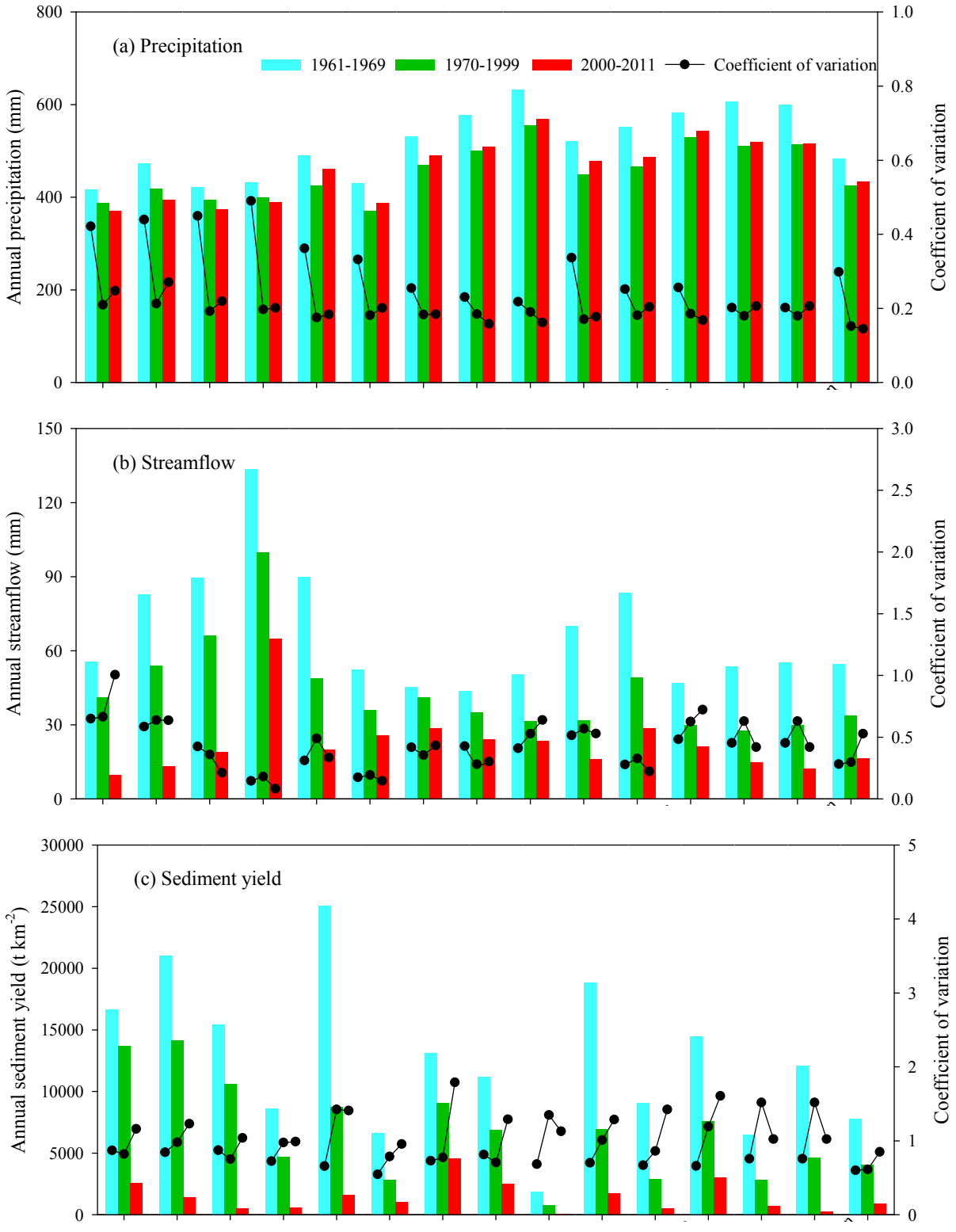
(a) Precipitation
1961-1969
1970-1999
2000-2011
Coefficient of variation
Annual precipitation (mm)
Coefficient of variation
(b) Streamflow
Annual streamflow (mm)
Coefficient of variation
(c) Sediment yield
Annual sediment yield (t km-2)
Coefficient of variation

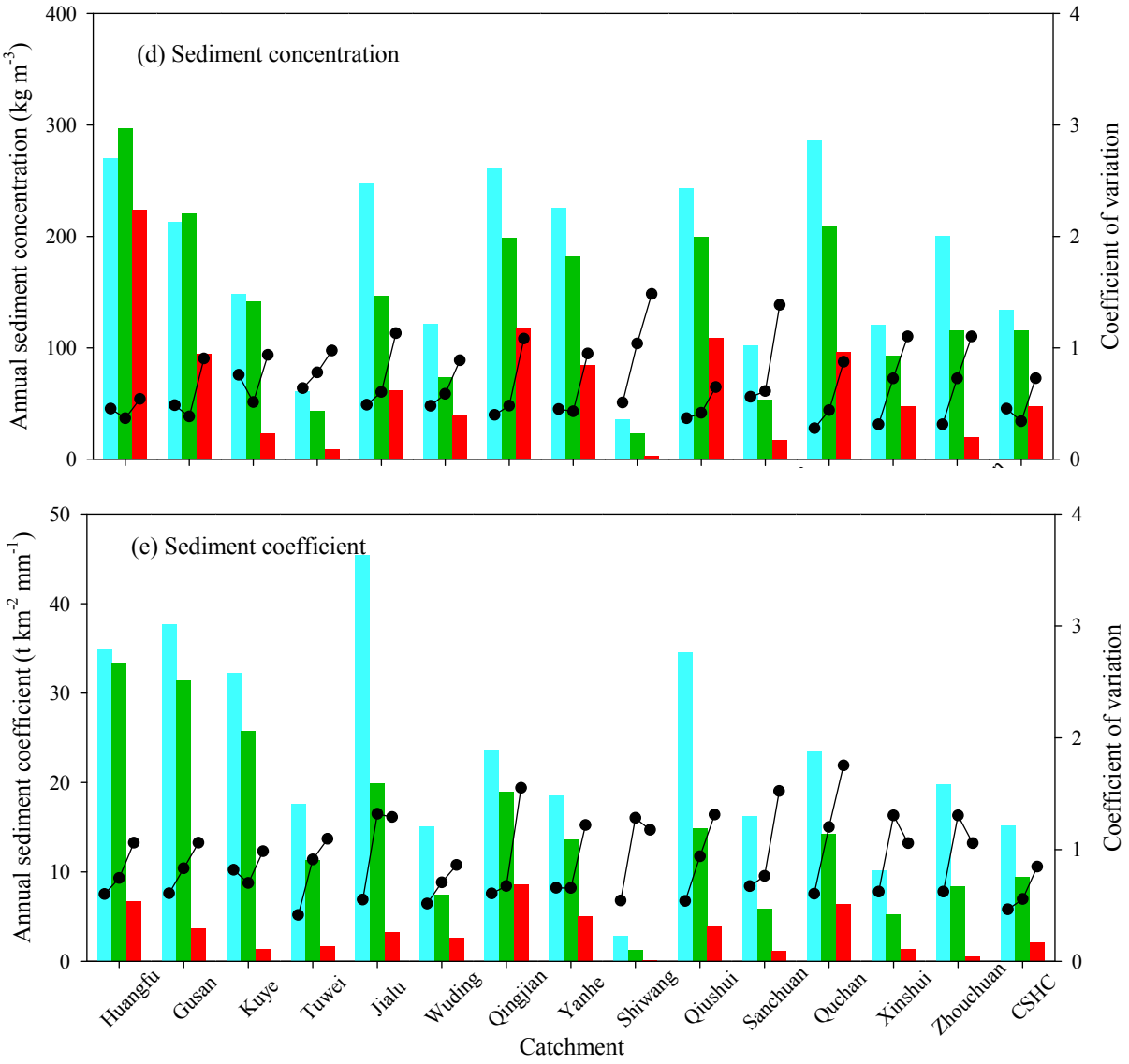

Figure 7. The changes of (a) precipitation, (b) streamflow, (c) sediment yield, (d) sediment concentration and (e) sediment coefficient during different stages (1961-1969, 1970-1999 and 2000-2011).

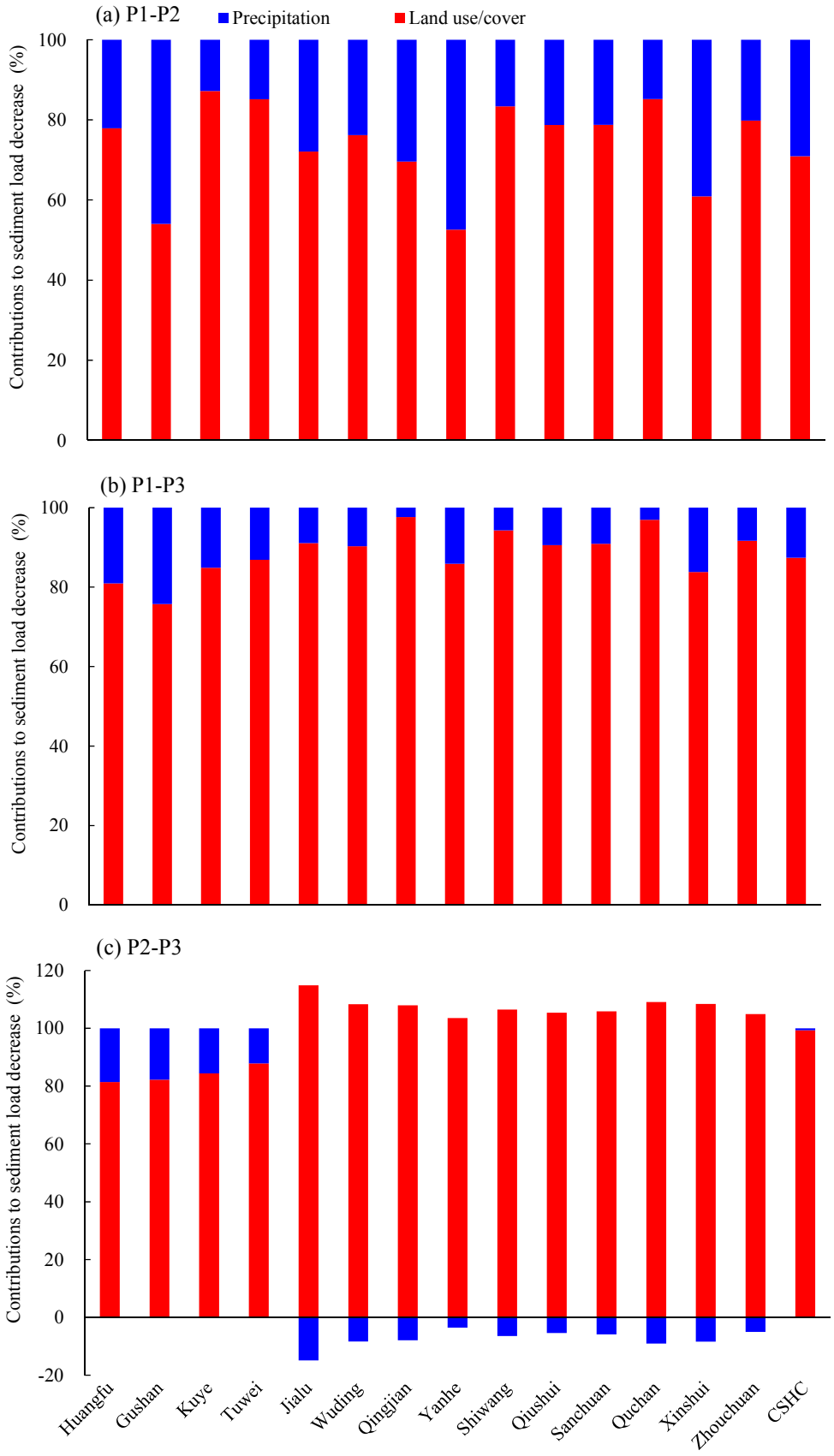

Figure 8. Contributions of precipitation and land use/cover to reductions of sediment load from (a) reference period (P1) to period-2 (P2), (b) reference period (P1) to period-3 (P3) and (c) period-2 (P2) to period-3 (P3).

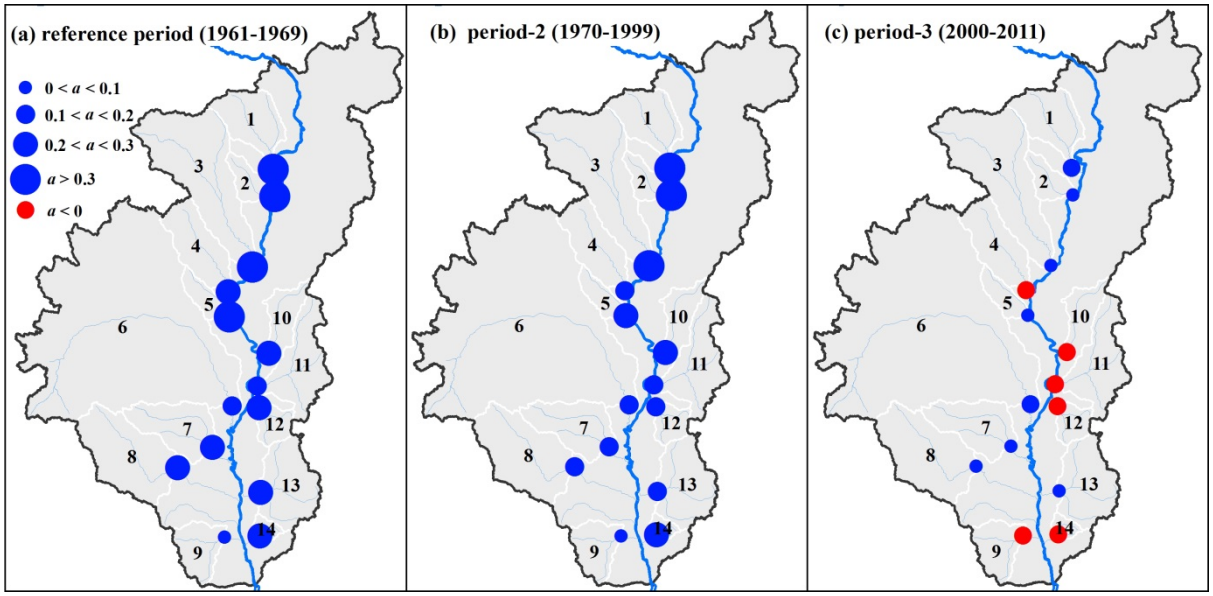

Figure 9. Spatial distribution of slope a in the regression equation $\sqrt{SSY} = aP + b$ during (a) reference period (1961-1969), (b) period-2 (1970-1999) and (c) period-3 (2000-2011). *SSY* is specific sediment yield, and *P* is precipitation.

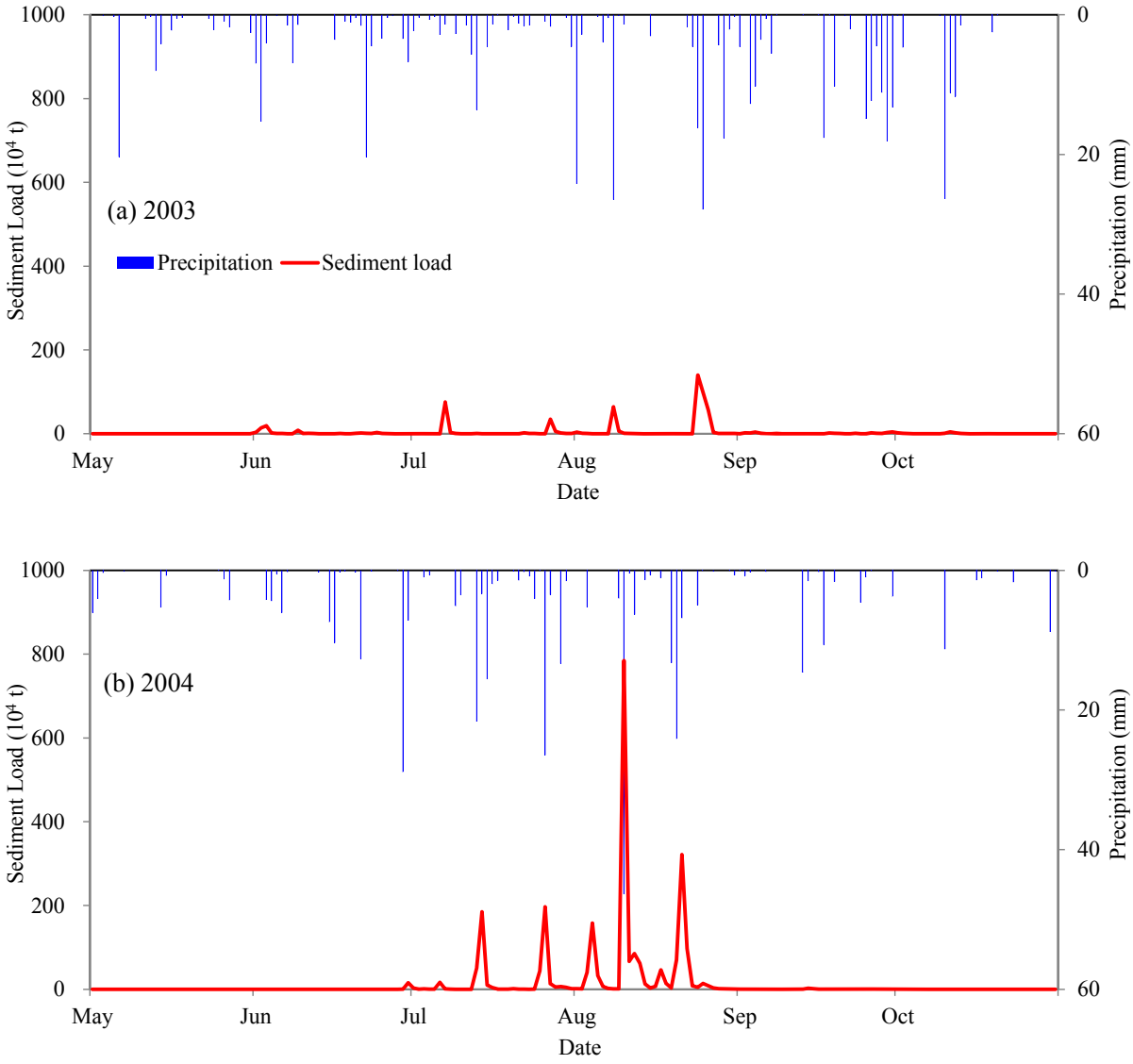

Figure 10. Daily precipitation and sediment load of the Yanhe catchment during rainy season (May-October) in (a) 2003 and (b) 2004.

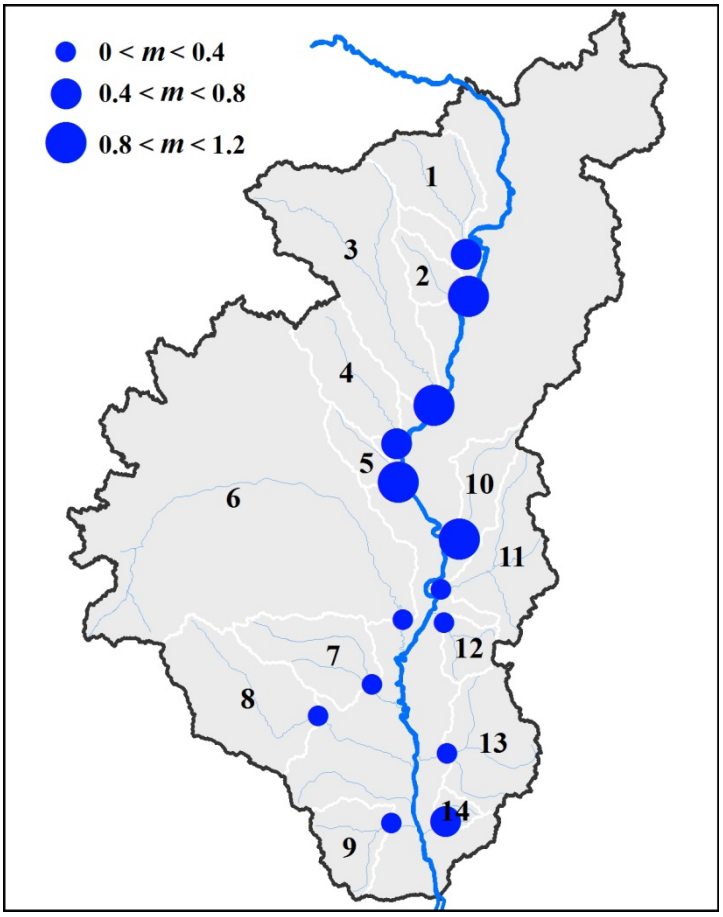

Figure 11. Spatial distribution of slope m in the regression equation $\overline{SC} = -mA_c + n$. $\overline{SC}$ is the decadal average sediment coefficient, and A_c is the percentage of the area affected by soil and water conservation measures in the catchments.